Italian Association of Aeronautics and Astronautics
XXVII AIDAA Congress
4-7 September 2023, Padova, Italy

Trajectory optimization and multiple-sliding-surface terminal guidance in the lifting atmospheric reentry

EDOARDO MARIA LEONARDI[1,a *] and MAURO PONTANI[2,c]

[1]Department of Astronautical, Electrical, and Energy Engineering, Sapienza University of Rome, via Salaria 851, 00138 Rome, Italy

[a]edoardomaria.leonardi@uniroma1.it, [b]mauro.pontani@uniroma1.it

Keywords: lifting reentry, optimal guidance, sliding-mode.

Abstract. In this paper the problem of guiding a vehicle from the entry interface to the ground is addressed. The Space Shuttle Orbiter is assumed as the reference vehicle and its aerodynamics data are interpolated in order to properly simulate its dynamics. The transatmospheric guidance is based on an open-loop optimal strategy which minimizes the total heat input absorbed by the vehicle while satisfying all the constraints. Instead, the terminal phase guidance is achieved through a multiple-sliding-surface technique, able to drive the vehicle toward a specified landing point, with desired heading angle and vertical velocity at touchdown, even in the presence of nonnominal initial conditions. The time derivatives of lift coefficient and bank angle are used as control inputs, while the sliding surfaces are defined so that these two inputs are involved simultaneously in the lateral and vertical guidance. The terminal guidance strategy is successfully tested through a Monte Carlo campaign, in the presence of stochastic winds and wide dispersions on the initial conditions at the Terminal Area Energy Management, in more critical scenarios with respect to the orbiter safety criteria.

Introduction

The development of an effective guidance architecture for atmospheric reentry and precise landing represents a crucial issue for the design of reusable vehicles capable of performing safe planetary reentry. Unsurprisingly, the interest in guidance and control technologies for atmospheric reentry and landing of winged vehicles has increased [1-2], as the flexibility and controllability of the reentry trajectory can be increased through the employment of lifting bodies. However, this implies a greater sensitivity to the environmental conditions. Thus, the usefulness of a real-time guidance algorithm, able to generate online trajectories, is evident, for the purpose of guaranteeing safe descent and landing even in the presence of nonnominal conditions and dispersions caused by the preceding transatmospheric phase.

The guidance and control strategy of the Space Shuttle relied on the modulation of the bank angle to follow a pre-computed reference drag profile, and could only account for small deviations from the nominal conditions [3]. Mease and Kremer and Mease et al. [4] revisited the Shuttle reentry guidance, using nonlinear geometric methods. Later on, Benito and Mease [5] developed and applied a new controller based on model prediction, where the bank angle is modulated to minimize an effective cost function which accounts for the error in drag acceleration and downrange. Nonlinear predictive control was employed by Minwen and Dayi to generate skip entry trajectories for low lift-to-drag vehicles [6]. Most recently, Lu [7] considered a unified guidance methodology based on a predictor-corrector algorithm, for vehicles with

different aerodynamic efficiency, while satisfying the boundaries on the thermic flux and load factor. Instead, a more limited number of papers addressed the terminal descent and landing, which is traveled after the Terminal Area Energy Management (TAEM) interface. Kluever [8] developed a guidance scheme for an unpowered vehicle with limited normal acceleration capabilities. Bollino et al. [9] employed a pseudospectral-based algorithm for optimal feedback guidance of reentry spacecraft, in the presence of large uncertainties and disturbances. Fahroo and Doman [10] used again a pseudospectral method in a mission scenario with actuation failures. Finally, reinforcement learning was used for autonomous guidance algorithms for precise landing [11]. Recently, sliding mode control was proposed as an effective nonlinear approach to yield real-time feedback control laws able to drive an unpowered space vehicle toward a specified landing site [3,12]. Depending on the instantaneous state and the desired final conditions, sliding mode control was already shown to be effective for generating feasible atmospheric paths leading to safe landing in finite time, even when several nonnominal flight conditions may occur that can significantly deviate the vehicle from the desired trajectory, e.g. winds or atmospheric density fluctuations [13].

In this work, an open-loop optimal guidance is developed for the transatmospheric arc, capable of minimizing the total heat input while driving the vehicle toward the TAEM. The Space Shuttle Orbiter is taken as the reference vehicle and an analytical method is employed to keep the maximum thermic flux below the safety limit, while accounting for the saturation on the control variables. Finally, the multiple-sliding-surface guidance is employed in order to drive the vehicle from the TAEM to the landing point, with accurate aerodynamic modelling, while including stochastic winds and large dispersions on the initial values of the state and control variables.

Reentry dynamics

The reentry vehicle is modelled as a 3-DOF lifting body and the position of the centre of mass is identified by a set of three spherical coordinates (r, λ_g, φ), representing respectively the instantaneous radius, the geographical longitude and the latitude. The additional variables are given by the relative velocity with respect to the Earth surface v_r, the heading angle ζ_r and the flight path angle γ_r. The trajectory equations describe the motion of the center of mass due to the effect of the forces acting on it [14].

The Space Shuttle Orbiter is taken as the reference vehicle for numerical simulations. It is assumed that the lift and drag coefficients (C_L and C_D) depend only on the angle of attack α and Mach number M, while the sideslip coefficient C_Q depends only of the sideslip angle β and Mach number M. The aerodynamics coefficients are obtained from wind tunnel tests [15] and are interpolated in order to derive their expressions as continuous functions of the aerodynamic angles and Mach number ($C_L = C_L(\alpha, M)$, $C_D = C_D(\alpha, M)$, $C_Q = C_Q(\beta, M)$).

Transatmospheric phase

The transatmospheric guidance drives the vehicle from the entry interface towards the TAEM, while keeping the thermic flux per unit area at the stagnation point q_s below the maximum value and minimizing the cost function

$$J = k_r \Delta_r + k_y \Delta_y + k_z \Delta_z + k_v \Delta_v + k_\zeta \Delta_\zeta + k_\gamma \Delta_\gamma + k_q \int_0^{t_f} q_s \, dt \tag{1}$$

where the coefficients k are chosen to balance the different contributions, while the terms Δ represent the deviations on the state variables at the final time, located at the TAEM. The reentry

trajectory is sampled at equally-spaced time instants t_k from the entry interface to the TAEM and the guidance law is determined through parametric optimization of the following parameters:

- sampled values of the bank angle;
- sampled values of the angle of attack from $M = 6$ to the TAEM;
- the total time of flight t_f from the reentry interface to the TAEM;
- the Mach number M^* at the end of the costant-angle-of-attack flight profile;
- the argument of latitude u_0 at the initial time;

The boundary conditions reflect the typical discent profile of the Space Shuttle [16] ($r_0 = 122000$ m, $v_{r0} = 7300$ m/s, $\gamma_{r0} = -1.4°$, $r_f = 25000$ m, $v_{rf} = 762$ m/s, $\varphi_f = 29.41°$, $\lambda_g = -81.46°$, $\zeta_f = -60.24°$) and the algorithm must keep the thermic flux below the maximum allowable value, equal to 681.39 kW/m^2, even lower than the typical value reported in the scientific literature, i.e. 794.43 kW/m^2 [17]. The dynamic pressure must be less than 16.375 kPa.

Thermic flux saturation. The thermic flux at the leading edge can be computed as $q_s = q_a q_r$, where $q_r = a\sqrt{\rho}(bv_r)^n$ and $q_a = c_0 + c_1\alpha + c_2\alpha^2 + c_3\alpha^3$, with a = 17700, b = 0.0001 and n = 3.07 [17]. The derivative of the thermic flux can be easily computed as $\dot{q}_s = Fq_a + q_r G\dot{\alpha}$, where F and G are auxiliary functions that do not depend on the input variable ($\dot{\alpha}$). Therefore, the time derivative of the lift coefficient can be computed as

$$\dot{C}_L = \frac{dC_L}{d\alpha}\dot{\alpha} = -\frac{dC_L}{d\alpha}\frac{F}{G}\frac{q_a}{q_r} \tag{2}$$

Guidance strategy. The descent of the vehicle through the atmosphere is controlled through modulation of the angle of attack and bank angle. In particular, the variation of the angle of attack follows the succession of four distinct flight profiles:

- constant-angle-of-attack flight from the entry interface to $M = M^*$;
- variable-angle-of-attack flight as described by Eq. 10;
- variable-angle-of attack flight following a sinusoidal profile from $M = M^*$ to $\tilde{M} = 6$;
- variable-angle-of-attack flight optimized by the guidance algorithm.

Numerical results. Table 1 reports the results of the optimization. The guidance algorithm is able to drive the vehicle through the atmosphere, with limited dispersions on the final state at the TAEM (cf. Table **1**), along a descent path close to the actual trajectory of the Orbiter [16].

Table 1: displacements of the state variables from the boundary values at TAEM

Q [MJ/m^2]	Δr [m]	Δy [m]	Δz [m]	Δv_r [m/s]	$\Delta\zeta_r$ [°]	$\Delta\gamma_r$ [°]
325.87	2.05	0.32	53.95	9.50	$6.35 \cdot 10^{-4}$	$1.26 \cdot 10^{-5}$

Fig. ***1*** and 2 highlight the time history of the angle of attack, which keeps the thermic flux below the maximum value. Saturation of the thermal flux occurs after about 200 s, as shown

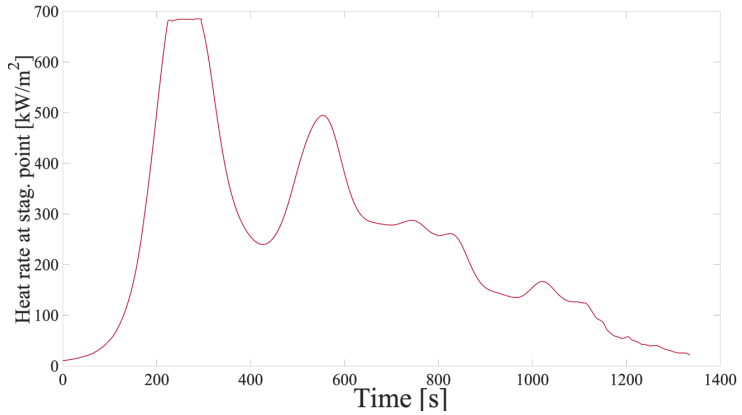

Fig. 1: time histories of the thermal flux along the transatmospheric arc

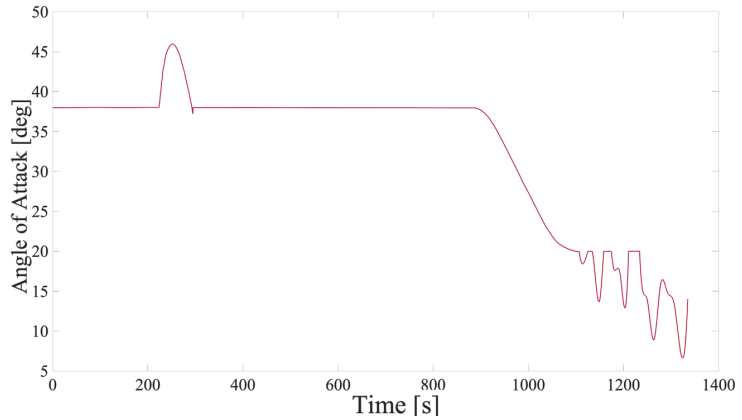

Fig. 2: time histories of the angle of attack along the transatmospheric arc

Terminal guidance

Along the transatmospheric arc, different factors may modify the reentry trajectory from the reference profile. Therefore, the terminal guidance must be able to drive the vehicle despite a wide range of initial conditions. In a previous work, sliding-mode control was already employed as a nonlinear approach to yield real-time feedback guidance laws in an accurate dynamic framework, including winds and large deviations from the initial trajectory variables [13]. In this study, significant improvements are developed with respect to the previous research:

- sliding-mode guidance is tested for a longer time period (i.e. from the TAEM to ground) and the aerodynamic modeling is based on real data rather than approximate analytical expressions;
- the saturation of the control variables is accounted inside the expression of the control input, so that only feasible trajectories are generated;
- the guidance gains are updated through an adaptive strategy, allowing further extension of the capability of the algorithm.

Numerical results. A total number of 500 simulations are run and the initial conditions are randomly generated with upper/lower bounds set to $\pm 2\sigma_s$ (where σ_s denotes the standard deviation of the variable of interest). Stochastic wind is also accounted for, whose intensity and direction is stronger than the safety limits prescribed for the Space Shuttle Orbiter landing [18]. Table **2** collects the initial conditions and associated standard deviations, which reflect the actual reference flight profile of the Space Shuttle [16]. Instead, Table **3** collects the results of the Monte Carlo campaign.

Table 2: initial conditions and standard deviations

Variable	$x(0)$ [m]	$y(0)$ [m]	$z(0)$ [m]	$v_r(0)$ [m/s]	$\zeta_r(0)$ [deg]	$\gamma_r(0)$ [deg]	$C_L(0)$ [-]	$\sigma(0)$ [deg]
Initial Conditions	24050	-54850	95932	762	ζ_f	-8	0.3969	0
Std. Dev.	0	2500	2500	15	5	1	0.01	5

Table 3: results of the Montecarlo campaign

Variable	r_{down} [m]	r_{cross} [m]	$\dot{x}$ [m/s]	v_r [m/s]	ζ_r [deg]	γ_r [deg]	α [deg]	σ [deg]
Mean	761.61	4.41	-1.02	138.69	-60.23	-0.43	6.26	-0.07
Std. Dev.	$-5.66 \cdot 10^{-3}$	$5.04 \cdot 10^{-3}$	0.10	16.63	0.02	0.09	1.74	1.17

From inspection of Table 3, it is evident that the algorithm is able to drive the vehicle to the prescribed landing point, which is located 762 m beyond the runway threshold, with limited crossrange component and vertical velocity at touchdown, and the proper alignment with the runway [16]. Figure 3 shows the stream of trajectories from the TAEM to the landing runway.

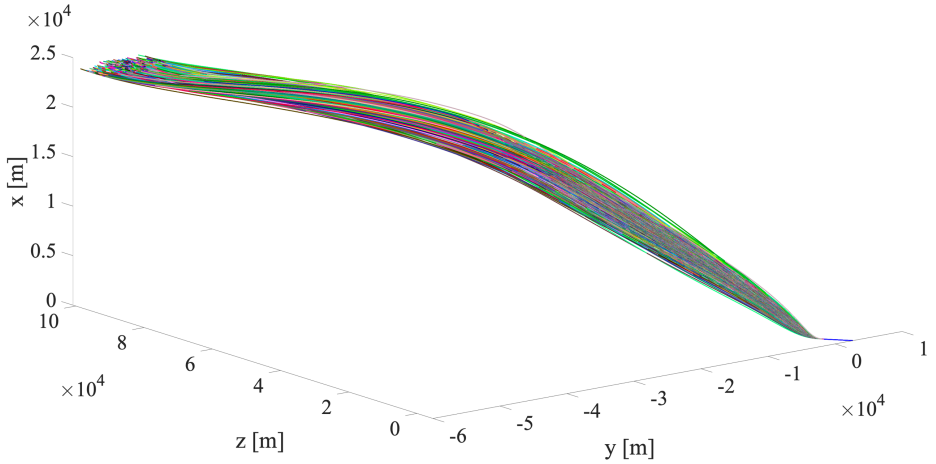

Fig. 3: stream of trajectories

Concluding remarks

This paper addresses the problem of driving a winged vehicle (i.e. the Space Shuttle Orbiter) from the entry interface to landing, while satisfying all the constraints. The transatmospheric guidance is based on an open-loop algorithm that minimizes the total heat input and saturates the maximum thermic flux. The terminal guidance is based on a multiple-sliding-surface strategy, which allows online generation of trajectories. The simulation setup includes a complete dynamic framework with an accurate aerodynamics modeling based on wind tunnel tests. The numerical results show the ability of the proposed guidance to modulate the angle of attack to avoid exceeding the maximum thermal flux, while compensating for winds and dispersions of position and velocity from the nominal trajectory during the terminal phase. The vehicle reaches the landing point with the proper alignment with the runway and a safe vertical velocity.

References

[1] R. Haya, L. T. Castellani and A. Ayuso, "Reentry GNC concept for a reusable orbital platform (space rider)", *69th International Astronautical Congress,* Bremen, Germany, *IAC-18 D*, Vol. 2, 2018, p. 5.

[2] Z. Krevor, R. Howard, T. Mosher and K. Scott, "Dream Chaser Commercial Crewed Spacecraft Overview", *17th AIAA International Space Planes and Hypersonic Systems and Technologies Conference,* AIAA Paper 2011-2245, 2011.

[3] N. Harl and S. Balakrishnan, "Reentry terminal guidance through sliding mode control", *Journal of Guidance, Control and Dynamics,* Vol. 33, No. 1, pp. 186-199, 2010.

[4] K. D. Mease and J.-P. Kremer, "Shuttle Entry Guidance Revisited Using Nonlinear Geometric Methods", *Journal of Guidance, Control and Dynamics,* Vol. 17, No. 6, 1994, pp. 1350-1356.

[5] J. Benito and K. D. Mease, "Nonlinear Predictive Controller for Drag Tracking in Entry Guidance", *AIAA/AAS Astrodynamics Specialist Conference and Exhibit,* AIAA Paper 2008-7350, 2008.

[6] G. Minwen and W. Dayi, "Guidance Law for Low-Lift Skip Reentry Subject to Control Saturation Based on Nonlinear Predictive Control", *Aerospace Science and Technoogy,* Vol. 37, No. 6, 2014, pp. 48-54.

[7] P. Lu, "Entry Guidance: A Unified Method", *Journal of Guidance, Control and Dynamics,* Vol. 37, No. 3, 2014, pp. 713-728.

[8] C. A. Kluever, "Unpowered Approach and Landing Guidance Using Trajectory Planning", *Journal of Guidance, Control and Dynamics,* Vol. 27, No. 6, 2004, pp. 967-974.

[9] M. R. K. Bollino and D. Doman, "Optimal Nonlinear Feedback Guidance for Reentry Vehicles", *AIAA Guidance, Navigation and Control Conference and Exhibit,* AIAA Paper 2006-6074, 2006.

[10] F. Fahroo and D. Doman, "A Direct Method for Approach and Landing Trajectory Reshaping with Failure Effect Estimation", *AIAA Guidance, Navigatin and Control Conference and Exhibit,* AIAA Paper 2004-4772, 2004.

[11] B. Gaude, R. Linares and R. Furfaro, "Deep reinforcement learning for six degree-of-freedom planetary landing", *Advances in Space Research*, Vol. 65, No. 7, pp. 1723-1741, 2020.

[12] X. Liu, F. Li, Y. Zhao, "Approach and Landing Guidance Design for Reusable Launch Vhicle Using Multiple Sliding Surfaces Techniques", *Chinese Journal of Aeronautics*, Vol. 30, No. 4, 2017, pp. 1582-1591.

[13] A. Vitiello, E. M. Leonardi and M. Pontani, "Multiple-Sliding-Surface Guidance and Control for Terminal Atmospheric Reentry and Precise Landing", *Journal of Spacecraft and Rockets*, Vol. 60, N. 3, pp. 912-923, 2023.

[14] M. Pontani, *Advanced Spacecraft Dynamics*, 1st ed., Edizioni Efesto, Rome, 2023, pp. 253-259.

[15] C. Weiland, *Aerodynamic Data of Space Vehicles,* 1st ed., Springer Berlin, Heidelberg, 2014, pp. 174-197.

[16] D. R. Jenkins, *Space Shuttle: The History of the National Space Transportation System: The First 100 Missions*, D. R. Jenkins, Cape Canaveral, 2008, pp. 260-261.

[17] J. T. Betts, *Practical methods for optimal control and estimation using nonlinear programming,* 2nd ed., SIAM, Philadelphia, 2010, pp. 247-256.

[19] S. Siceloff, "Nasa-Space Shuttle Weather Launch Commit Criteria and KSC End of Mission Weather Landing Criteria", 2003.